2001

Polymer depletion interaction between two parallel repulsive walls

F. Schlesener

Andreas Hanke
The University of Texas Rio Grande Valley

R. Kimpel

S. Dietrich

Recommended Citation

Schlesener, F., et al. "Polymer Depletion Interaction between Two Parallel Repulsive Walls." Physical Review E, vol. 63, no. 4, American Physical Society, Mar. 2001, p. 041803, doi:10.1103/PhysRevE.63.041803.

Polymer depletion interaction between two parallel repulsive walls

F. Schlesener,[1,2] A. Hanke,[3] R. Klimpel,[1] and S. Dietrich[2,4]
[1]*Fachbereich Physik, Bergische Universität Wuppertal, D-42097 Wuppertal, Germany*
[2]*Max-Planck-Institut für Metallforschung, Heisenbergstrasse 1, D-70569 Stuttgart, Germany*
[3]*Department of Physics, Massachusetts Institute of Technology, Cambridge, Massachusetts 02139*
[4]*Institut für Theoretische und Angewandte Physik, Universität Stuttgart, D-70550 Stuttgart, Germany*
(Received 23 October 2000; published 27 March 2001)

The depletion interaction between two parallel repulsive walls confining a dilute solution of long and flexible polymer chains is studied by field-theoretic methods. Special attention is paid to self-avoidance between chain monomers relevant for polymers in a good solvent. Our direct approach avoids the mapping of the actual polymer chains on effective hard or soft spheres. We compare our results with recent Monte Carlo simulations [A. Milchev and K. Binder, Eur. Phys. J. B **3**, 477 (1998)] and with experimental results for the depletion interaction between a spherical colloidal particle and a planar wall in a dilute solution of nonionic polymers [D. Rudhardt, C. Bechinger, and P. Leiderer, Phys. Rev. Lett. **81**, 1330 (1998)].

DOI: 10.1103/PhysRevE.63.041803 PACS number(s): 61.25.Hq, 61.41.+e, 68.35.Rh, 82.70.Dd

I. INTRODUCTION

In polymer solutions the overlap of depletion zones for monomers due to repulsive confining walls or mesoscopic particles dissolved in the solution induces an important and tunable effective interaction potential [1]. For example, this depletion interaction successfully explains phase diagrams of colloid-polymer mixtures [2–4]. Recent experimental techniques facilitate even the measurement of the depletion force between a wall and a *single* colloidal particle [5–7]. In the context of such solutions confined to thin films and porous materials the geometry of two parallel walls has been extensively studied as a paradigmatic case [8–14].

For strongly overlapping chains as realized in a *semidilute* polymer solution, chain flexibility is taken into account within self-consistent field theory or within the framework of phenomenological scaling theory [15–17]. On the other hand, in a *dilute* polymer solution different chains do not overlap so that the behavior of the polymer solution is determined by the behavior of a single chain. To a certain extent and under certain circumstances, a single chain can be modeled by a random walk without self-avoidance (ideal chain). In three dimensions this situation is closely realized in a so-called θ-solvent [18]. If the solvent temperature is below the θ-point (poor solvent) the polymer coils tend to collapse [19,20]. However, in the common case that the solvent temperature is above the θ-point (good solvent) the excluded volume (EV) interaction between chain monomers becomes relevant so that the polymer coils are less compact than the corresponding ideal chains. The emphasis in this work is on the latter situation and we investigate the effect of the EV interaction on the depletion interaction between two parallel walls as compared to the case of confined ideal chains.

By focusing on *long* flexible chains in a system of mesoscopic size we obtain mostly *universal* results that are independent of microscopic details [18,21–26]. Due to the universality of the corresponding properties it is sufficient to choose a simple model for calculating these results. For our investigations we use an Edwards-type model [18,21,22] for the polymer chain, which allows for an expansion in terms of the EV interaction and is amenable to a field-theoretical treatment via the polymer magnet analogy. The basic elements in this expansion are partition functions $\mathcal{Z}_{\mathrm{seg}}^{[0]}(\mathbf{r},\mathbf{r}')$ for chain segments that have no EV interaction (as indicated by the superscript $[0]$) and with the two ends of the segment fixed at $\mathbf{r}$ and $\mathbf{r}'$. This perturbative treatment has to be carried out in the presence of confining geometries. We consider two structureless parallel walls in d dimensions and a distance D apart so that in coordinates $\mathbf{r}=(\mathbf{r}_\parallel,z)$ the surface of the bottom wall is located at $z=0$ and $\mathbf{r}_\parallel$ comprises the $d-1$ components of $\mathbf{r}$ parallel to the walls. The surface of the upper wall is located at $z=D$. The interaction of the polymer with the nonadsorbing walls is implemented by the boundary condition that the segment partition function and thus the partition function for the whole chain vanishes as any segment approaches the surface of the walls [18,23], i.e.,

$$\mathcal{Z}_{\mathrm{seg}}^{[0]}(\mathbf{r},\mathbf{r}')\to 0, \quad z,z'\to 0,D. \tag{1.1}$$

For the present purpose the only relevant property that characterizes one of the polymer chains is its mean square end-to-end distance in the bulk solution, which we denote by $d\mathcal{R}_x^2$ [24–26]; for convenience we include the spatial dimension d as a prefactor. The results presented in the following are obtained for $d=3$ both for ideal chains and for chains with EV interaction. In Sec. II we present our results for the interaction potential and the force between two parallel walls. We note that for chains with EV interaction these results are valid only in the limit $D\gg\mathcal{R}_x$ because our theoretical approach is not capable of describing the dimensional crossover to the behavior of a quasi-$(d-1)$-dimensional system which arises for $D\ll\mathcal{R}_x$. In Sec. III we compare these results with the simulation data of Milchev and Binder [14]. In Sec. IV we apply the Derjaguin approximation in order to obtain from the results in Sec. II the depletion interaction between a spherical particle and a wall in a dilute polymer solution and compare it with the corresponding experimental results of Rudhardt, Bechinger, and Leiderer [6].

In view of the complexity of the actual experimental systems involving spatially confined colloidal suspensions dis-

solved in a solution containing polymers, in the past the corresponding theoretical descriptions relied on suitable coarse-grained, effective models and on integrating out less relevant degrees of freedom. The gross features of these systems can be obtained by mapping the polymers onto effective hard spheres as pioneered by Asakura and Oosawa [27]. In a more refined description Louis *et al.* [28,29] derived effective interaction potentials between polymer coils such that they behave like soft spheres. This approach allows one to capture the crossover in structural properties to semidilute and dense polymer solutions. Based on such a model Louis *et al.* [29] have calculated, among other things, the corresponding depletion energy between two parallel repulsive plates. Besides presenting the depletion energy for ideal chains in terms of an expansion introduced by Asakura and Oosawa, they find the occurrence of repulsive depletion forces in an intermediate regime of D upon significantly increasing the polymer density. In our present completely analytic study we focus on dilute polymer solutions, for which the depletion forces turn out to be always attractive, by fully taking into account the flexibility of the polymer chains and the self-avoidance of the polymer segments with a particular emphasis on long chains. This complementary point of view allows us to make contact with the Monte Carlo simulation data in Ref. [14] and with the experimental data in Ref. [6]; these comparisons have not been carried out before to our knowledge.

II. EFFECTIVE INTERACTION BETWEEN PARALLEL WALLS

A. Grand canonical ensemble

In a dilute polymer solution the interaction between N different chains can be neglected so that the total free energy of the system is N times the free energy of a single chain. We consider the polymer solution within the slit to be in equilibrium contact with an equivalent polymer solution in a reservoir outside the slit so that there is exchange of polymer coils between the slit and the reservoir. The *free energy of interaction* between the walls in such a grand canonical ensemble is given by

$$\delta F = -k_B T N \left\{ \ln\left(\frac{\mathcal{Z}_{||}(D)}{\mathcal{Z}} \right) - \ln\left(\frac{\mathcal{Z}_{||}(D=\infty)}{\mathcal{Z}} \right) \right\}, \quad (2.1)$$

where $\mathcal{Z}_{||}(D)$ is the partition function of one polymer chain in a large volume $\mathcal{V}$ containing the walls and $\mathcal{Z}$ is the corresponding partition function of one polymer chain in the volume $\mathcal{V}$ without the walls. In the thermodynamic limit $\mathcal{V}\to\mathbb{R}^d$ one has [24–26]

$$\mathcal{Z} \to \mathcal{V}\hat{\mathcal{Z}}_b \quad (2.2)$$

with $\hat{\mathcal{Z}}_b = \int_{\mathbb{R}^d} d^d r'\, \mathcal{Z}_b(\mathbf{r},\mathbf{r}')$ and where $\mathcal{Z}_b(\mathbf{r},\mathbf{r}')$ denotes the partition function of one polymer chain in the unbounded solution with its ends fixed at $\mathbf{r}$ and $\mathbf{r}'$. Correspondingly, $\mathcal{Z}_{||}(\mathbf{r},\mathbf{r}')$ denotes the partition function of one polymer chain within the volume $\mathcal{V}$ containing the parallel walls and with its ends fixed at $\mathbf{r}$ and $\mathbf{r}'$. The volume $\mathcal{V}=\mathcal{V}_I+\mathcal{V}_O$ can be divided into the volume $\mathcal{V}_I$ within the slit and the volume $\mathcal{V}_O$ outside the slit. Since the polymer chain cannot penetrate the walls, whose lateral extensions are large, $\mathcal{Z}_{||}(\mathbf{r},\mathbf{r}')$ is nonzero only if both $\mathbf{r}$ and $\mathbf{r}'$ are in $\mathcal{V}_I$ or in $\mathcal{V}_O$ so that

$$\begin{aligned} \mathcal{Z}_{||}(D) &= \int_{\mathcal{V}} d^d r \int_{\mathcal{V}} d^d r'\, \mathcal{Z}_{||}(\mathbf{r},\mathbf{r}') \\ &= \int_{\mathcal{V}_O} d^d r\, \hat{\mathcal{Z}}_O(z) + \int_{\mathcal{V}_I} d^d r\, \hat{\mathcal{Z}}_I(z), \end{aligned} \quad (2.3)$$

with $\hat{\mathcal{Z}}_{O,I}(z) = \int_{\mathcal{V}_{O,I}} d^d r'\, \mathcal{Z}_{||}(\mathbf{r},\mathbf{r}')$. In the thermodynamic limit $\mathcal{V}\to\mathbb{R}^d$ the logarithm $\ln(\mathcal{Z}_{||}/\mathcal{Z})$ in Eq. (2.1) can be expanded using Eqs. (2.2) and (2.3), i.e.,

$$\begin{aligned} \ln\left(\frac{\mathcal{Z}_{||}(D)}{\mathcal{Z}} \right) &= \ln\left(1 + \frac{\mathcal{Z}_{||}(D) - \mathcal{Z}}{\mathcal{Z}} \right) \\ &\to \frac{1}{\mathcal{V}} \frac{\mathcal{Z}_{||}(D) - \mathcal{V}\hat{\mathcal{Z}}_b}{\hat{\mathcal{Z}}_b} \\ &= \frac{1}{\mathcal{V}} \left[\int_{\mathcal{V}_O} d^d r \left(\frac{\hat{\mathcal{Z}}_O(z)}{\hat{\mathcal{Z}}_b} - 1 \right) \right. \\ &\quad \left. + \int_{\mathcal{V}_I} d^d r \left(\frac{\hat{\mathcal{Z}}_I(z)}{\hat{\mathcal{Z}}_b} - 1 \right) \right], \end{aligned} \quad (2.4)$$

where the ratio $(\mathcal{Z}_{||}(D) - \mathcal{Z})/\mathcal{Z}$ is of the order $\mathcal{V}_I/\mathcal{V}$, which tends to zero because the slit width D is fixed. Since in the thermodynamic limit the leading contribution to the first integral of Eq. (2.4) is independent of the slit width D we find for Eq. (2.1)

$$\begin{aligned} \delta F = -n_p k_b T \left\{ \int_{\mathcal{V}_I} d^d r \left(\frac{\hat{\mathcal{Z}}_I(z)}{\hat{\mathcal{Z}}_b} - 1 \right) \right. \\ \left. - \int_{\mathcal{V}_I} d^d r \left(\frac{\hat{\mathcal{Z}}_I(z)}{\hat{\mathcal{Z}}_b} - 1 \right) \Bigg|_{D=\infty} \right\}, \end{aligned} \quad (2.5)$$

with the number density $n_p = N/\mathcal{V}$ of the polymer chains in the bulk solution. The second integral in Eq. (2.5) reduces to the sum of two half-space (HS) integrals which yield contributions proportional to the area A of the walls [25]:

$$\begin{aligned} \int_{\mathcal{V}_I} d^d r \left(\frac{\hat{\mathcal{Z}}_I(z)}{\hat{\mathcal{Z}}_b} - 1 \right) \Bigg|_{D=\infty} &= 2 \int_{\mathrm{HS}} d^d r \left(\frac{\hat{\mathcal{Z}}_{\mathrm{HS}}(z)}{\hat{\mathcal{Z}}_b} - 1 \right) \\ &= -2A \frac{\Delta\sigma}{n_p k_B T}, \end{aligned} \quad (2.6)$$

where we have introduced the surface tension $\Delta\sigma$ between the polymer solution and the confining wall [compare Eqs. (1.7) and (2.41) in Ref. [25]]. Note that the mean polymer density within the slit is determined by the bulk density n_p, i.e., in the grand canonical ensemble the chemical potential

μ of the polymer coils is fixed instead of the number N_I of polymer coils in the slit (see Sec. II B).

According to Eqs. (2.5) and (2.6) the total grand canonical free energy Ω of the polymer solution within the slit,

$$\Omega = -n_p k_B T A D \omega, \tag{2.7}$$

with the dimensionless quantity

$$\omega = \frac{1}{D}\int_0^D dz \frac{\hat{\mathcal{Z}}_I(z)}{\hat{\mathcal{Z}}_b}, \tag{2.8}$$

can be decomposed as

$$\frac{\Omega}{n_p k_B T A} = D f_b + 2 f_s + \delta f. \tag{2.9a}$$

On the right-hand side (rhs) of Eq. (2.9a) appear the reduced bulk free energy per unit volume

$$f_b = -1, \tag{2.9b}$$

the reduced surface free energy per unit area

$$f_s = \frac{\Delta\sigma}{n_p k_B T}, \tag{2.9c}$$

and the reduced free energy of interaction

$$\delta f = \frac{\delta F}{n_p k_B T A}. \tag{2.9d}$$

B. Canonical ensemble

If instead of the chemical potential μ the number N_I of polymer coils in the slit is used as independent variable, the total free energy F of the polymer solution within the slit in the canonical ensemble follows from Ω as the Legendre transform

$$F(N_I) = \Omega[\mu(N_I)] + \mu(N_I) N_I, \tag{2.10}$$

where Ω is given by Eq. (2.7). The chemical potential μ is related to n_p via [30]

$$\mu = k_B T \ln(n_p \Lambda^d), \tag{2.11}$$

where Λ is the thermal de Broglie wave length of the particles, i.e., polymer coils. Equation (2.7) implies for dilute solutions

$$N_I = -\frac{\partial\Omega(\mu)}{\partial\mu} = \frac{-n_p}{k_B T}\frac{\partial\Omega}{\partial n_p} = \frac{-\Omega}{k_B T}. \tag{2.12}$$

Thus $F(N_I)$ is given by

$$F(N_I) = -k_B T N_I + k_B T N_I \ln\left(\frac{N_I}{A D \omega}\Lambda^d\right) \tag{2.13}$$

with ω from Eq. (2.8).

C. Free energy of interaction and mean force

We employ the polymer magnet analogy [18,21–25] in order to calculate the partition functions $\hat{\mathcal{Z}}_{\rm HS}(z)$, $\hat{\mathcal{Z}}_I(z)$, and $\hat{\mathcal{Z}}_b$ as needed in Eqs. (2.5), (2.6), and (2.8) for a single chain with EV interaction. They are functions of the parameter u_0 which characterizes the strength of the EV interaction and L_0 which determines the number of monomers of the chain such that L_0 equals $\mathcal{R}_g^2 = \mathcal{R}_x^2/2$ for an ideal chain in the bulk, i.e., for $u_0 = 0$. The well-known arguments of the polymer magnet analogy [18,21–23] imply for the present case the correspondence

$$\mathcal{Z}_{||}(\mathbf{r},\mathbf{r}';L_0,D,u_0) = \mathcal{L}_{t_0\to L_0}\langle\Phi_1(\mathbf{r})\Phi_1(\mathbf{r}')\rangle\big|_{\mathcal{N}=0} \tag{2.14}$$

between $\mathcal{Z}_{||}(\mathbf{r},\mathbf{r}')$ and the two-point correlation function $\langle\Phi_1(\mathbf{r})\Phi_1(\mathbf{r}')\rangle$ in an $O(\mathcal{N})$ symmetric field theory for an $\mathcal{N}$-component order parameter field $\mathbf{\Phi} = (\Phi_1, \ldots, \Phi_{\mathcal{N}})$ in the restricted volume $\mathcal{V}_I$. In Eq. (2.14) the operator

$$\mathcal{L}_{t_0\to L_0} = \frac{1}{2\pi i}\int_{\mathcal{C}} dt_0\, e^{L_0 t_0} \tag{2.15}$$

acting on the correlation function is an inverse Laplace transform with $\mathcal{C}$ a path in the complex t_0 plane to the right of all singularities of the integrand. The Laplace conjugate t_0 of L_0 and the excluded volume strength u_0 appear, respectively, as the ''temperature'' parameter and as the prefactor of the $(\Phi^2)^2$ term in the Ginzburg-Landau Hamiltonian,

$$\mathcal{H}\{\mathbf{\Phi}\} = \int_V d^d r\left\{\frac{1}{2}(\boldsymbol{\nabla}\mathbf{\Phi})^2 + \frac{t_0}{2}\mathbf{\Phi}^2 + \frac{u_0}{24}(\mathbf{\Phi}^2)^2\right\}, \tag{2.16}$$

which provides the statistical weight $\exp(-\mathcal{H}\{\mathbf{\Phi}\})$ for the field theory. The requirement in Eq. (1.1) describing the repulsive character of the walls imposes the Dirichlet condition

$$\mathbf{\Phi}(\mathbf{r}) = 0, \quad z = 0, D, \tag{2.17}$$

on both walls. This corresponds to the fixed point boundary condition of the so-called ordinary transition [31,32] for the field theory. For the renormalization group improved perturbative investigations we use a dimensionally regularized continuum version of the field theory, which we shall renormalize by minimal subtraction of poles in $\varepsilon = 4 - d$ [33]. The basic element of the perturbation expansion is the Gaussian two-point correlation function (or propagator) $\langle\Phi_i(\mathbf{r})\,\Phi_j(\mathbf{r}')\rangle_{[0]}$ where the subscript $[0]$ denotes $u_0 = 0$ [see Eq. (A1) in the Appendix].

The loop expansion to first order in u_0 and the renormalization of ω in Eq. (2.8) are completely analogous to the outline in Sec. II A of Ref. [25]. Some key results of this procedure relevant for the present case are given in the Appendix. The final results for f_s and δf on the rhs of Eq. (2.9a) are given by Eqs. (A5) and (A6) in the Appendix, where $\mathcal{N} = 0$ for the present polymer case and $\varepsilon = 1$ in $d = 3$.

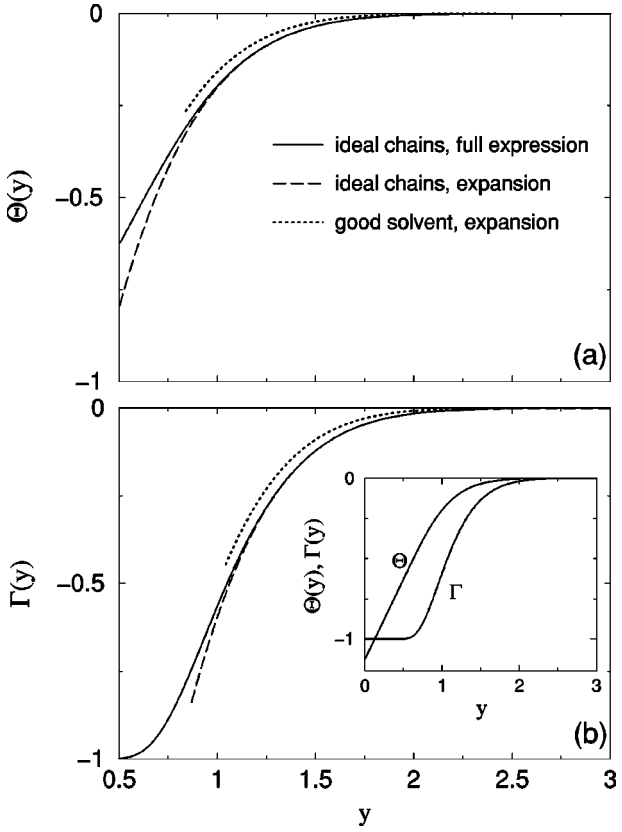

FIG. 1. Scaling functions (a) $\Theta(y)$ for the depletion interaction potential and (b) $\Gamma(y)=-d\Theta/dy$ for the depletion force between two repulsive, parallel plates at a distance D confining a dilute polymer solution in terms of the scaling variable $y=D/\mathcal{R}_x$ [see Eqs. (2.18) and (2.19)]. $\mathcal{R}_x=\sqrt{2}\,\mathcal{R}_g$ for ideal chains and $\mathcal{R}_x=1.444\,\mathcal{R}_g$ in a good solvent for a bulk solution [see Eqs. (4.2) and (4.3) below], where $\mathcal{R}_g$ is the radius of gyration. For ideal chains the full expression, which is valid in the whole range of y (solid line; see also the inset), and an expansion of this expression, which is valid for $y\gtrsim 1$ (dashed line), are shown. The same expansion is shown for chains in a good solvent (dotted line). The dotted line stops where the dashed line starts to deviate appreciably from the solid line.

Figure 1 shows the universal scaling function for the free energy of interaction

$$\Theta(y)=\frac{1}{\mathcal{R}_x}\,\delta f \tag{2.18}$$

with δf from Eq. (2.9d) and the corresponding scaling function for the force

$$\Gamma(y)=-\frac{\mathrm{d}\Theta(y)}{\mathrm{d}y} \tag{2.19}$$

in terms of the scaling variable

$$y=D/\mathcal{R}_x\,. \tag{2.20}$$

Figure 1 shows both the behavior for ideal chains and for chains with EV interaction. For chains with EV interaction the present theoretical approach can only capture the behavior for $D/\mathcal{R}_x$ large, i.e., $y\gg 1$. As expected the depletion potential and the resulting force are *weaker* for chains with EV interaction than for ideal chains, because the EV interaction effectively reduces the depletion effect of the walls. The inset of Fig. 1 shows both Θ and Γ for ideal chains. The narrow slit limits read

$$\Theta(y\to 0)=-\frac{2}{\sqrt{\pi}}+y \tag{2.21}$$

and

$$\Gamma(y\to 0)=-1. \tag{2.22}$$

Deviations from the linear behavior in Eq. (2.21) become visible only for $y\gtrsim\frac{1}{2}$. In the opposite limit $y\to\infty$ the leading behavior for ideal chains is given by

$$\Theta(y\to\infty)=-4\sqrt{\frac{2}{\pi}}\frac{1}{y^2}e^{-y^2/2} \tag{2.23}$$

and

$$\Gamma(y\to\infty)=-4\sqrt{\frac{2}{\pi}}\frac{1}{y}e^{-y^2/2}. \tag{2.24}$$

The depletion potential in terms of the scaling function $\Theta(y)$ is attractive. But whether the bulk contribution Df_b has to be taken into account in addition depends on the ''experimental'' setup. In the case that the force is measured between plates immersed in a container filled with the dilute polymer solution such that solvent and polymer coils can freely enter the slit from the reservoir, only the scaling functions Θ and Γ are relevant. This is also true for the particle-wall geometry discussed in Sec. IV. But if no exchange is allowed, as for the Monte Carlo simulation discussed in Sec. III, the force $\mathcal{K}$ defined in Eq. (3.2) is needed.

III. COMPARISON WITH MONTE CARLO SIMULATIONS

Monte Carlo simulations of polymers are well established both for ideal chains and for chains with self-avoidance. In this section we compare our results with the simulation of a polymer chain between two repulsive walls by Milchev and Binder [14] which corresponds to the case studied theoretically here. These authors use a bead spring model for the self-avoiding polymer chain with a short-ranged repulsive interaction between the beads.

In Refs. [9] and [14] (see in particular Fig. 4 in Ref. [14]) it is stated that the total force $\mathcal{K}$ between the two walls is repulsive and diverges in the narrow slit limit, i.e.,

$$\frac{D\mathcal{K}}{k_BT}\propto\left(\frac{D}{\mathcal{R}_g}\right)^{-1/\nu}, \tag{3.1}$$

where $\nu=\frac{1}{2}$ for ideal chains and $\nu=0.588$ for chains with EV interaction, and $\mathcal{R}_g$ is the radius of gyration of the polymer chain in unbounded space [14]. [For the definition of $\mathcal{R}_g$ see Eqs. (4.2) and (4.3) in Sec. IV.] The qualitative differ-

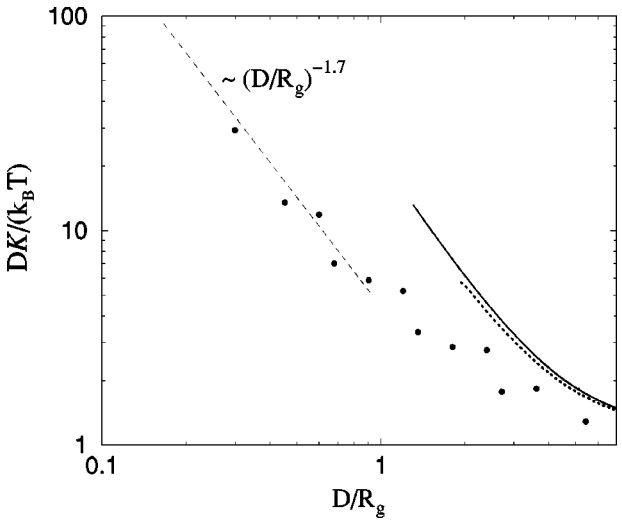

FIG. 2. Depletion force $\mathcal{K}$ [Eq. (3.2)] between two parallel walls at distance D confining repulsively a dilute polymer solution. $\mathcal{R}_g$ is the radius of gyration of the chains [see Eqs. (4.2) and (4.3)]. The solid circles correspond to the Monte Carlo simulation data in Ref. [14]. The force obtained from Eq. (3.2) is shown for ideal chains (solid line) and self-avoiding chains (dotted line). The latter line stops where the expansion for large $D/\mathcal{R}_g$ turns out to become unreliable. The dashed line represents the asymptotic behavior at small distances for chains in a good solvent [see Eq. (3.1)], with a fit for the amplitude of the power-law behavior. For $D/\mathcal{R}_g \to \infty$ the reduced force $D\mathcal{K}/(k_BT)$ tends to 1.

ence from the scaling function $\Gamma(y)$ presented for the force in Sec. II C is explained by the following arguments. (a) The total force between the walls is repulsive due to the contribution from the cost in free energy caused by the loss of the total available space for the polymer chains within the slit, i.e., the bulk pressure $-f_b$ contributes to the total force. (b) The total force $\mathcal{K}$ diverges due to the change from the grand canonical to the canonical ensemble (see Sec. II B). In the simulation in Ref. [14] the number N_I of polymers in the slit is given by one polymer in the slit volume. Therefore we obtain the total force $\mathcal{K}$ by differentiating Eq. (2.13) with respect to the slit width D and by setting $N_I=1$, i.e.,

$$\frac{D\mathcal{K}}{k_BT} = \frac{1}{\omega}\frac{\mathrm{d}}{\mathrm{d}D}(D\,\omega), \tag{3.2}$$

where $D\,\omega = -\Omega/(n_p k_B T A)$ is given by the rhs of Eq. (2.9a) in conjunction with Eqs. (A5) and (A6) in Appendix A. The lhs of Eq. (3.2) corresponds to the quantity Df in Ref. [14].

Figure 2 shows comparison of the simulation data of Ref. [14] and the corresponding theoretical result from Eq. (3.2), the latter for both ideal chains and chains with EV interaction. Note that the theoretical curve for chains with EV interaction is valid only for large $D/\mathcal{R}_g$. The curve for chains with EV interaction is closer to the simulation data than the curve for ideal chains, in agreement with the fact that the polymer chain in the simulation is a self-avoiding one. One possible reason for the remaining deviation might be that the chain in the simulation is too short to be fully described by the present field-theoretical approach. The deviation of the Monte Carlo simulation data at large values of $D/\mathcal{R}_g$ from the power-law behavior at small values of $D/\mathcal{R}_g$ (dashed line) occurs because $D\mathcal{K}/k_BT$ tends to 1 for large $D/\mathcal{R}_g$, which is not captured by Eq. (3.1).

Figures 5–9 of Ref. [14] show density profiles for the simulated chains with EV interaction, including a comparison with the analytical result for the profile of ideal chains in the slit (Fig. 9 in Ref. [14]). We want to mention here that the field-theoretical treatment of the monomer density for chains with EV interaction requires a perturbation expansion involving integrals over $G\times G\times G\times G$ instead of $G\times G\times G$ (see the Appendix) and thus in view of the technical challenges is beyond the scope of the present study. Alternative information about the monomer density profiles beyond the ideal behavior can be found in Ref. [34] in which a self-consistent mean-field approximation is used to obtain the monomer density profiles for a single polymer chain between two repulsive walls.

IV. COMPARISON WITH EXPERIMENT

Rudhardt, Bechinger, and Leiderer [6] have measured the depletion interaction between a wall and a colloidal particle immersed in a dilute solution of nonionic polymer chains in a good solvent by means of total internal reflection microscopy (TIRM). They monitored the fluctuations of the relative distance of the colloid particle from the wall induced by Brownian motion. From the resulting Boltzmann distribution one can infer the corresponding effective depletion potential between the repulsive wall and the particle.

In order to compare these experimental data with our results we apply the Derjaguin approximation [35]. In the limit that the radius R of the spherical particle is much larger than both $\mathcal{R}_x$ and the distance a of closest approach surface to surface between the particle and the wall, the particle can be regarded as composed of a pile of fringes. Each fringe builds a fringelike slit with distance $D=a+r_{||}^2/2R$, where $r_{||}$ is the radius of the fringe. Thus the interaction between the particle and the wall is given by

$$\frac{\Phi_{\mathrm{depl}}(a)}{n_p k_B T} = 2\pi R\,\mathcal{R}_x^2 \int_0^\infty d\upsilon\,\upsilon\,\Theta\left(\frac{a}{\mathcal{R}_x}+\frac{\upsilon^2}{2}\right), \tag{4.1}$$

where υ is a dimensionless variable and $\Theta(y)$ is the scaling function for the free energy of interaction for the slit geometry [see Eq. (2.18)].

In Ref. [6] the interaction potential $\Phi_{\mathrm{depl}}(a)$ is measured for nonionic polymer chains in a good solvent for polymer number densities $n_p=0$, 7.6, 10.2, 12.7, and 25.5 $\mu\mathrm{m}^{-3}$. All these polymer number densities represent a *dilute* polymer solution so that $\Phi_{\mathrm{depl}}(a)$ is a linear function of n_p [see Eq. (2.1)]. Therefore our results are applicable and Fig. 3 shows Φ_{depl}/n_p as a function of a. The crosses in Fig. 3 correspond to those values of a for which the above mentioned linear behavior $\Phi_{\mathrm{depl}} \propto n_p$ (not shown) is in good agreement with the experimental data. Deviations from the linear behavior $\Phi_{\mathrm{depl}} \propto n_p$ for small and large particle-wall distances a (not shown) can be explained by the experimental method TIRM

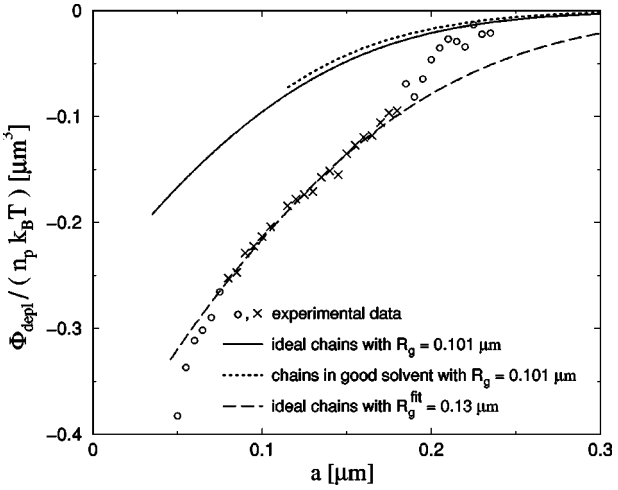

FIG. 3. Depletion interaction potential $\Phi_{\mathrm{depl}}(a)$ between a spherical colloidal particle immersed in a dilute polymer solution and the container wall as a function of the distance a of closest approach surface to surface between the sphere and the wall [see Eq. (4.1)]. The interaction potential is given in units of k_BT and of the polymer number density n_p. The circles and crosses indicate the experimental data from Ref. [6]. Crosses show the range where the linear relationship $\Phi_{\mathrm{depl}} \propto n_p$ allows for a direct comparison with the theoretical results. The theoretically calculated depletion interaction is shown for ideal chains (solid line) and chains in a good solvent (dotted line) as realized in the experiment. These curves correspond to the value $\mathcal{R}_g = 0.101$ μm, which has been determined by independent experiments [see Eqs. (4.2) and (4.3)]. Using the radius of gyration as a fit parameter yields the dashed line corresponding to $\mathcal{R}_g = 0.13$ μm and ideal chains.

used in Ref. [6]: a higher interaction potential implies a lower probability of finding the particle at the corresponding distance, causing lower accuracy. It turns out that the total interaction potential as the sum of depletion potential, electrostatic repulsion, and gravity is highest for short and large distances, which are those where the linear relationship $\Phi_{\mathrm{depl}} \propto n_p$ is not confirmed experimentally. Figure 3 also shows the corresponding theoretical predictions for the experimental data, for both ideal polymer chains and chains with EV interaction, i.e., chains in a good solvent as realized in the experiment. Note that all parameters entering these theoretical predictions are *fixed* by available experimental data for n_p, a, and $\mathcal{R}_g$, i.e., there are no freely adjustable parameters. In particular, the radius of gyration $\mathcal{R}_g$ of the polymer chains used in Ref. [6] has been measured fairly accurately by means of small angle scattering of x rays [36], resulting in $\mathcal{R}_g = 0.101$ μm. According to the definition of $\mathcal{R}_g$ as measured in small angle scattering experiments [37], i.e.,

$$\mathcal{R}_g^2 = \frac{\int d^3r \int d^3r' \rho(\mathbf{r})\rho(\mathbf{r}')|\mathbf{r}-\mathbf{r}'|^2}{2\int d^3r \int d^3r' \rho(\mathbf{r})\rho(\mathbf{r}')}, \tag{4.2}$$

where $\rho(\mathbf{r})$ is the monomer density, in $d=3$ one has [38]

$$\mathcal{R}_g = 0.6927\,\mathcal{R}_x, \quad d=3. \tag{4.3}$$

Figure 3 shows that the experimental data of Ref. [6] deviate from the theoretical result derived here. Note that this deviation is not visible if the polymer size is used as a freely adjustable parameter in order to gain agreement between the experimental and theoretical data. The theoretical curve for chains with EV interaction, as realized in the experiment, is even *further away* from the experimental data than the theoretical curve for ideal chains. The latter observation confirms the necessity of reinterpreting the experimental data, e.g., by adjusting the radius of gyration. This can be done such that agreement with the theoretical data for chains with EV interaction is gained for the intermediate values of the distance where the linear relationship $\Phi_{\mathrm{depl}} \propto n_p$ allows for a direct comparison with the theory. [The remaining differences outside this intermediate regime ($\bigcirc$) pose a separate issue as discussed in the paragraph following Eq. (4.1).] However, the difference between the two theoretical curves for ideal chains and chains with EV interaction is small compared to the deviation from the experimental data.

Any attempt to use the Monte Carlo data obtained in Ref. [14] for predicting the depletion interaction between a colloidal particle and a wall would require two integrations of $\mathcal{K}$ and a change to the grand canonical ensemble, which poses prohibitive accuracy problems. Nonetheless, a qualitative statement can be given easily. Figure 2 shows that the force obtained in the Monte Carlo simulation is weaker than the force calculated for chains with EV interaction. This is also expected to hold for the depletion interaction between a particle and the wall.

V. CONCLUDING REMARKS AND SUMMARY

Based on field-theoretical techniques we have determined the effective depletion interaction between two nonadsorbing walls confining a dilute solution of long flexible polymer chains. Our main results are the following.

(1) The field-theoretical calculation yields the universal scaling functions of the depletion interaction potential and the corresponding force for ideal chains and for chains with excluded volume interaction in the limit $y = D/\mathcal{R}_x \gg 1$, where D is the separation between the walls and $\mathcal{R}_x$ is the projected end-to-end distance of the chains [see Eqs. (2.18), (2.19), and (4.3) and Fig. 1]. The depletion potential is weaker for chains in a good solvent than for ideal chains.

(2) For $y \gtrsim 1$ we find fair agreement with corresponding Monte Carlo simulation data [14] if the excluded volume interaction is taken into account (see Fig. 2). We surmise that remaining discrepancies are due to higher order terms in the field-theoretical calculation which are not yet taken into account, and due to the possibility that the length of the simulated polymer chain has not yet reached the scaling limit for which the field theory is valid.

(3) Using the Derjaguin approximation we have compared our theoretical results with the experimental data [6] for the depletion potential between a spherical colloidal particle and a wall (see Fig. 3). We obtain a fair agreement only if the radius of gyration $\mathcal{R}_g$ of the polymers is used as a fit param-

eter. This value, however, differs from independently determined values for $\mathcal{R}_g$. The reasons for these differences are not yet understood. The excluded volume interaction between the monomers of the polymer chain plays only a minor role for reaching agreement between theory and experiment.

ACKNOWLEDGMENTS

We thank A. Milchev and K. Binder for a helpful discussion of their simulation data and C. Bechinger for providing the experimental data. This work has been supported by the German Science Foundation through both Sonderforschungsbereich 237 ''Unordnung und große Fluktuationen'' and the graduate college ''Feldtheoretische und numerische Methoden der Elementarteilchen- und Statistischen Physik.''

APPENDIX

The Gaussian two-point correlation function in the slit of width D reads

$$\begin{aligned}\langle \Phi_i(\mathbf{r})\,\Phi_j(\mathbf{r}')\rangle_{[0]} &= \delta_{ij}\,G(\mathbf{r},\mathbf{r}';t_0,D)\\ &= \delta_{ij}\,\hat{G}(|\mathbf{r}_\parallel-\mathbf{r}'_\parallel|,z,z';t_0,D)\\ &= \delta_{ij}\int\frac{d^{d-1}p}{(2\pi)^{d-1}}\exp[i\mathbf{p}\cdot(\mathbf{r}_\parallel-\mathbf{r}'_\parallel)]\tilde{G}(\mathbf{p},z,z';t_0,D),\end{aligned} \tag{A1}$$

with the Gaussian propagator $\tilde{G}(\mathbf{p},z,z';t_0,D)$ in p-z representation given by [32,39]

$$\begin{aligned}\tilde{G}(\mathbf{p},z,z';t_0,D) &= \frac{1}{2b}\left[e^{-b|z-z'|}-e^{-b(z+z')}+\frac{e^{-b(z-z')}+e^{-b(z'-z)}}{e^{2bD}-1}\right.\\ &\quad\left.-\frac{e^{-b(z+z')}+e^{b(z+z')}}{e^{2bD}-1}\right],\end{aligned} \tag{A2}$$

where $b=\sqrt{p^2+t_0}$. The loop expansion of the total susceptibility reads [40]

$$\begin{aligned}\chi(t_0,D,u_0) &= \int_0^D dz dz'\tilde{G}(\mathbf{0},z,z')-\frac{u_0}{2}\frac{\mathcal{N}+2}{3}\int_0^D dz dz' dz''\\ &\quad\times\int\frac{d^{d-1}p}{(2\pi)^{d-1}}\tilde{G}(\mathbf{0},z,z'')\tilde{G}(\mathbf{p},z'',z'')\\ &\quad\times\tilde{G}(\mathbf{0},z'',z')+O(u_0^2).\end{aligned} \tag{A3}$$

The procedure outlined in Sec. II A of Ref. [25] yields the renormalized total susceptibility in one-loop order as (see also Appendix B of Ref. [40]):

$$\begin{aligned}\chi_{\rm ren}[\tau=(D\mu)^2t,D,u]/D^3 &= \frac{1}{\tau}-\frac{2}{\tau^{3/2}}\frac{1-e^{-\sqrt{\tau}}}{1+e^{-\sqrt{\tau}}}+u\frac{\mathcal{N}+2}{3}\frac{2}{\tau^{3/2}}\left\{\left[\sqrt{\tau}+2\sqrt{\tau}\,\frac{e^{-\sqrt{\tau}}}{(1+e^{-\sqrt{\tau}})^2}-3\frac{1-e^{\sqrt{\tau}}}{1+e^{\sqrt{\tau}}}\right]\right.\\ &\quad\times\left[2f_1+2\ln(D\mu)-\ln\tau+\ln(4\pi)+1-C_E-8\int_1^\infty ds\,\frac{\sqrt{s^2-1}}{e^{2\sqrt{\tau}s}-1}\right]\\ &\quad-4\pi\frac{1/2-1/\sqrt{3}+e^{-\sqrt{\tau}}(2-\sqrt{3})+e^{-2\sqrt{\tau}}(1/2-1/\sqrt{3})}{(1+e^{-\sqrt{\tau}})^2}\\ &\quad\left.-4\frac{1-e^{-\sqrt{\tau}}}{1+e^{-\sqrt{\tau}}}\int_0^\infty ds\frac{\sqrt{s^2-1}}{e^{2\sqrt{\tau}s}-1}\left(\frac{2}{s+\frac{1}{2}}+\frac{2}{s-\frac{1}{2}}+\frac{1}{s-1}-\frac{1}{s+1}\right)\right\}+O(u^2).\end{aligned} \tag{A4}$$

Here μ is the inverse length scale which determines the renormalization group flow; t and u are the renormalized and dimensionless counterparts of t_0 and u_0, respectively; C_E is Euler's constant; and for the definition of the constant f_1 we refer to Ref. [25].

The free energy is obtained via the inverse Laplace transform of $\chi_{\rm ren}(D)$ and normalization by the transformed renormalized total susceptibility for the unbounded space $\chi_{{\rm ren},b}$. The decomposition into bulk, surface, and finite-size contributions is carried out by analysis of the scaling behavior of these parts of the free energy. The surface and finite-size parts of the free energy [see Eq. (2.9)] at the fixed point of the renormalization group and for $\mathcal{N}=0$ with the scaling variable $y=D/\mathcal{R}_x$ are given by

$$f_s = \mathcal{R}_x \sqrt{\frac{2}{\pi}} \left\{ 1 - \frac{\varepsilon}{4} \left[1 - \frac{3 \ln 2}{2} - \frac{\pi}{2} + \frac{\pi}{\sqrt{3}} \right] \right\} \quad \text{(A5)}$$

and

$$\begin{aligned} \frac{\delta f}{D} = {} & 4 \operatorname{erfc}\left(\frac{y}{\sqrt{2}} \right) - 4 \sqrt{\frac{2}{\pi}} \frac{1}{y} e^{-y^2/2} \\ & - \frac{\varepsilon}{4} \left[\frac{e^{-y^2/2}}{y\sqrt{2\pi}} \left(4 + \frac{4\pi}{\sqrt{3}} - 4\pi + 6 \ln(2y^2) - 6 C_E \right) \right. \\ & + \operatorname{erfc}\left(\frac{y}{\sqrt{2}} \right) \left(2\pi - \frac{2\pi}{\sqrt{3}} - 2 \ln(2y^2) + 2 C_E \right) \\ & \left. - \mathcal{L}_{\tau \to \frac{1}{2y^2}} \left\{ \frac{e^{-\sqrt{\tau}} \ln \tau}{\tau} \right\} - 3 \mathcal{L}_{\tau \to 1/2y^2} \left\{ \frac{e^{-\sqrt{\tau}} \ln \tau}{\tau^{3/2}} \right\} \right] \\ & + O(\varepsilon^2), \end{aligned} \quad \text{(A6)}$$

where χ_{ren} in Eq. (A4) is expanded for large plate separations D up to order $O(e^{-\sqrt{D^2 t}})$, because for small distances the correct behavior including the dimensional crossover cannot be obtained even for the full expression. But using the expansion has the additional benefit of yielding partly analytical results for the separations D of interest here. For $d = 3$, R_x is related to the radius of gyration $\mathcal{R}_g$ by Eq. (4.3). The full result for ideal chains for δf is given by Eq. (A4) for $u = 0$, i.e.,

$$\delta f = -D \mathcal{L}_{\tau \to 1/2y^2} \left\{ \frac{4}{\tau^{3/2}} \frac{1}{1 + e^{\sqrt{\tau}}} \right\}, \quad \text{(A7)}$$

which is valid for all y.

[1] For a review, see, e.g., *Colloid Physics*, Proceedings of the Workshop on Colloid Physics, University of Konstanz, Germany, 1995, edited by G. Nägele, B. DAguanno, and A. Z. Akcasu [Physica A **235**, 1 (1997)].

[2] P. R. Sperry, H. B. Hopfenberg, and N. L. Thomas, J. Colloid Interface Sci. **82**, 62 (1980).

[3] H. N. W. Lekkerkerker, Physica A **213**, 18 (1995).

[4] W. C. K. Poon, S. M. Ilett, and P. N. Pusey, Nuovo Cimento D **16**, 1127 (1994).

[5] Y. N. Ohshima, H. Sakagami, K. Okumoto, A. Tokoyoda, T. Igarashi, K. B. Shintaku, S. Toride, H. Sekino, K. Kabuto, and I. Nishio, Phys. Rev. Lett. **78**, 3963 (1997).

[6] D. Rudhardt, C. Bechinger, and P. Leiderer, Phys. Rev. Lett. **81**, 1330 (1998).

[7] R. Verma, J. C. Crocker, T. C. Lubensky, and A. G. Yodh, Phys. Rev. Lett. **81**, 4004 (1998).

[8] For reviews see, e.g., G. J. Fleer, M. A. Cohen-Stuart, J. M. J. H. Scheutjens, T. Cosgrove, and B. Vincent, *Polymers at Interfaces* (Chapman and Hall, London, 1993); I. Teraoka, Prog. Polym. Sci. **21**, 89 (1996).

[9] E. Eisenriegler, Phys. Rev. E **55**, 3116 (1997).

[10] P. Cifra and T. Bleha, Macromol. Theory Simul. **8**, 603 (1999).

[11] K. Hagita, S. Koseki, and H. Takano, J. Phys. Soc. Jpn. **68**, 2144 (1999).

[12] R. L. Jones, S. K. Kumar, D. L. Ho, R. M. Briber, and T. P. Russel, Nature (London) **400**, 146 (1999).

[13] J. B. Hooper, J. D. McCoy, and J. G. Curro, J. Chem. Phys. **112**, 3090 (2000); J. B. Hooper, M. T. Pileggi, J. D. McCoy, J. G. Curro, and J. D. Weinhold, *ibid.* **112**, 3094 (2000).

[14] A. Milchev and K. Binder, Eur. Phys. J. B **3**, 477 (1998); **13**, 607 (2000).

[15] J. F. Joanny, L. Leibler, and P. G. de Gennes, J. Polym. Sci., Polym. Phys. Ed. **17**, 1073 (1979).

[16] P. G. de Gennes, C. R. Seances Acad. Sci., Ser. B **288**, 359 (1979).

[17] T. Odijk, Macromolecules **29**, 1842 (1996); J. Chem. Phys. **106**, 3402 (1996).

[18] P. G. de Gennes, *Scaling Concepts in Polymer Physics* (Cornell University Press, Ithaca, NY, 1979).

[19] C. E. Cordeiro, J. Phys. Chem. Solids **60**, 1645 (1999).

[20] Y. Singh, S. Kumar, and D. Giri, J. Phys. A **32**, L407 (1999).

[21] J. des Cloizeaux and G. Jannink, *Polymers in Solution* (Clarendon, Oxford, 1990).

[22] L. Schäfer, *Excluded Volume Effects in Polymer Solutions as Explained by the Renormalization Group* (Springer, Heidelberg, 1998).

[23] E. Eisenriegler, *Polymers Near Surfaces* (World Scientific, Singapore, 1993); E. Eisenriegler, in *Field Theoretical Tools in Polymer and Particle Physics*, Vol. 508 of *Lecture Notes in Physics*, edited by H. Meyer-Ortmanns and A. Klümper (Springer, Heidelberg, 1998), p. 1.

[24] E. Eisenriegler, A. Hanke, and S. Dietrich, Phys. Rev. E **54**, 1134 (1996).

[25] A. Hanke, E. Eisenriegler, and S. Dietrich, Phys. Rev. E **59**, 6853 (1999).

[26] A. Bringer, E. Eisenriegler, F. Schlesener, and A. Hanke, Eur. Phys. J. B **11**, 101 (1999).

[27] S. Asakura and F. Oosawa, J. Chem. Phys. **22**, 1255 (1954); J. Polym. Sci. **33**, 183 (1958).

[28] M. Murat and K. Kremer, J. Chem. Phys. **108**, 4340 (1998); F. Eurich and P. Maass, e-print cond-mat/0008425.

[29] A. A. Louis, P. G. Bolhuis, J. P. Hansen, and E. J. Meijer, Phys. Rev. Lett. **85**, 2522 (2000); P. G. Bolhuis, A. A. Louis, J. P. Hansen, and E. J. Meijer, J. Chem. Phys. **114**, 4296 (2000).

[30] M. Plischke and B. Bergersen, *Equilibrium Statistical Physics* (World Scientific, Singapore, 1994).

[31] K. Binder, in *Phase Transitions and Critical Phenomena*, Vol. 8, edited by C. Domb and J. L. Lebowitz (Academic, London, 1983), p. 1.

[32] H. W. Diehl, in *Phase Transitions and Critical Phenomena*, Vol. 10, edited by C. Domb and J. L. Lebowitz (Academic, London, 1986), p. 75; H. W. Diehl, Int. J. Mod. Phys. B **11**, 3503 (1997).

[33] D. J. Amit, *Field Theory, the Renormalization Group, and*

Critical Phenomena (McGraw-Hill, New York, 1978); J. Zinn-Justin, *Quantum Field Theory and Critical Phenomena* (Clarendon, Oxford, 1989).
[34] F. Rother, J. Phys. A **32**, 1439 (1999).
[35] B. V. Derjaguin, Kolloid-Z. **69**, 155 (1934).
[36] K. Devanand and J. C. Selser, Macromolecules **24**, 5943 (1991).
[37] See, e.g., L. A. Feigin and D. I. Svergun, *Structure Analysis by Small-Angle X-Ray and Neutron Scattering* (Plenum Press, New York, 1987), Chap. 3; compare also Eq. (1) in Ref. [36].
[38] P. Grassberger, P. Sutter, and L. Schäfer, J. Phys. A **30**, 7039 (1997); note that $\mathcal{R}_x = \mathcal{R}_E / \sqrt{3}$.
[39] M. Krech, E. Eisenriegler, and S. Dietrich, Phys. Rev. E **52**, 1345 (1995).
[40] R. Klimpel and S. Dietrich, Phys. Rev. B **60**, 16 977 (1999).